Synthesis and Characterization of Eggshell-derived Hydroxyapatite for Dental Implant Applications

Jamiu Odusote[1], *Adekunle* Adeleke[2], Peter Ikubanni[3], Peter Omoniyi[4*], Tien-Chien Jen[4], G. Odedele[1], Jude Okolie[5], and Esther Akinlabi[6]

[1]Department of Materials and Metallurgical Engineering, University of Ilorin, Ilorin, Nigeria
[2]Department of Mechanical Engineering, Nile University of Nigeria, Abuja, Nigeria
[3]Department of Mechanical Engineering, Landmark University, Omu-Aran, Nigeria
[4]Department of Mechanical Engineering Science, University of Johannesburg, Johannesburg, South Africa
[5]Gallogly College of Engineering, University of Oklahoma, Oklahoma, United States
[6]Mechanical and Construction Engineering Department, Northumbria University, Newcastle, United Kingdom

Abstract. Hydroxyapatite (HAp) production from eggshells for dental implant purposes involved a novel approach utilizing a wet chemical precipitation technique. The eggshells, finely ground to a size below 250 µm, underwent calcination at a high temperature of 900°C for 2 hours. This thermal treatment facilitated the conversion of calcium carbonate into calcium oxide (CaO) while eliminating any organic components in the eggshell. To initiate the synthesis of HAp, a solution comprising 0.6 M phosphoric acid was added to the CaO dispersed in water. The resulting mixture was allowed to undergo aging at different time intervals ranging from 0 to 24 hours, promoting the formation of HAp. Subsequently, the HAp particles were oven-dried at 100°C for 2 hours to remove residual moisture. Finally, the dried particles were sintered at 1200°C in a muffle furnace to achieve the desired properties for dental implant applications. XRD peaks at 25, 33, 40, and 50° confirm the synthesized material as HAp. Vibrational modes of phosphate (PO_4^{3-}), hydroxyl (OH^-), and carbonate (CO_3^{2-}) groups indicate carbonated HAp. Synthesized HAp holds potential for biomedical applications.

1 Introduction

The human body and parts, including the tooth, degrade significantly in old age. Accidents, injuries, defects, disease, or decay can cause tooth damage. These damages can be restored by various means, including; dentures, fixed bridges, and dental implants. Biocompatible metal anchors, or dental implants, are surgically positioned beneath the gum line within the jaw bone. These implants function as artificial tooth roots and support prosthetic crowns when natural teeth are absent. Dental implants are the most natural-looking tooth replacement option and do not slip like dentures. Implants may be the right choice for someone missing one, multiple, or even all of their teeth. The healing period for non-union bone after placing root-form implants, which closely resemble the natural tooth root, varies between three to six months or longer, depending on the individual. This period is crucial for osseointegration,

*Corresponding author: omoniyi.po@unilorin.edu.ng

© The Authors, published by EDP Sciences. This is an open access article distributed under the terms of the Creative Commons Attribution License 4.0 (https://creativecommons.org/licenses/by/4.0/).

where the bone integrates and grows around the implant, establishing a robust structural foundation. Subsequently, a superstructure is attached to the implant using either cementation or a screw-tightening retention method [1].

A highly valuable inorganic biomaterial extensively employed in biomedical fields is hydroxyapatite (HA) [2]. HA belongs to the apatite family of ceramic minerals and is composed of calcium phosphate with the chemical formula $Ca_{10}(PO_4)_6(OH)_2$, occurring naturally. The human bone and teeth contain between 70 and 80% hydroxyapatite (inorganic component) and 20-30% other inorganic elements (largely collagen) [3]. Tooth enamel, predominantly composed of hydroxyapatite, is the primary constituent. Remarkably devoid of water, it is renowned as the hardest tissue within the human body. Enamel functions as a protective layer encompassing the entire anatomical crown of a tooth, safeguarding the underlying dentin structurally. [4,5]. According to Sopyan et al. [6], Hydroxyapatite ceramic exhibits exceptional bioactivity and has been extensively applied in the medical field in various forms, including porous, dense, and granular bodies. Primarily employed as a coating, hydroxyapatite-coated implants offer notable benefits such as accelerated bone healing at the interface, reduced metal corrosion, and enhanced strength in the bone-to-implant connection [1].

Eggshells are agricultural waste; tons of eggs are produced yearly. In Africa alone, 3 million tonnes of eggs were produced as of 2012. Among the nations in Africa, Nigeria holds the position of being the largest producer of eggs. Over the period from 2000 to 2012, it experienced an average annual growth rate of 4%. Consequently, the total output reached an impressive 640,000 tonnes during that period [7]. Using the FAO data, it can be implied that at least 330,000 tonnes of eggshells are wasted in Africa, and 70,400 tonnes of eggshells are left as waste yearly in Nigeria alone. Approximately 11% of the egg's overall weight can be attributed to the eggshell composition, comprising 94% calcium carbonate, 1% calcium phosphate, 4% organic matter, and 1% magnesium carbonate [8]. High amounts of calcium carbonate make eggshells a suitable calcium source as a starting material for producing hydroxyapatite for commercial use.

Several studies documented in the literature [3,8–11] have explored the synthesis of hydroxyapatite using chicken eggshells. However, most of the described approaches are associated with high costs, necessitating cumbersome equipment, generating excess waste and sludge, and involving time-consuming synthesis procedures, thereby rendering the process labor-intensive. Adeogun et al., [12] and Lee et al. [13] demonstrated the use of eggshell and phosphoric acid in a wet chemical route to synthesize highly sinterable nano-sized hydroxyapatite powders. Following the calcination of the raw eggshell, the resulting calcined eggshell was combined with phosphoric acid in different proportions. Subsequently, the samples underwent sintering and were subjected to characterization, encompassing the assessment of crystallinity and internal morphology.

Suksomran and Molloy [14] also employed a wet chemical precipitation technique to generate hydroxyapatite. Under ambient conditions, three different orthophosphate sources were used. A finely ground calcium carbonate ($CaCO_3$) powder was utilized to serve as a calcium source. Orthophosphoric acid (H_3PO_4), ammonium dihydrogen orthophosphate ($NH_4H_2PO_4$), and diammonium hydrogen orthophosphate ($(NH_4)_2(HPO_4)$ were employed as sources of orthophosphate. Careful mixing of the raw materials and reagents resulted in the formation of the desired product. Subsequent characterization involved the utilization of X-ray Diffraction, Fourier transforms infrared analysis, and scanning electron spectroscopy techniques. Notably, the XRD patterns exhibited a striking resemblance to the HAP reference data. The FTIR spectra of all samples displayed characteristic bands associated with the HAp structure. The observations further revealed that the morphology of the hydroxyapatite was characterized by clustered nanoparticles, showcasing irregular ovular and spherical shapes

with sizes below 1 m. Additionally, individual fine particles displaying spherical and semispherical configurations were also observed.

Various research investigations have explored diverse approaches for synthesizing hydroxyapatite from eggshells. Noteworthy methods encompass a combination of ball milling and heat treatment, as described by Wu et al. [15], along with implementing a chemical precipitation and calcination technique [16]; mechanochemical activation method [17,18]; calcium oxide and tricalcium phosphate and heat treatment method [19]; rapid microwave method [20]; Sol-gel technique [21,22]; wet chemical precipitation reaction [23]; hydrothermal method [24] and so on. However, the three-step wet chemical precipitation method generates only water as waste with shorter hours of synthesis. It is simple, convenient, and relatively economical for hydroxyapatite production. One of the notable benefits of synthesizing hydroxyapatite from eggshells lies in its ability to retain certain properties from the original raw materials, including pore structure and carbonated HA, among others. Nevertheless, challenges arise due to the inherent variability in the physical and chemical characteristics of the utilized raw materials [25]. This study aims to produce hydroxyapatite from eggshells through a three-step wet chemical precipitation method. Subsequently, the synthesized hydroxyapatite will be characterized using X-ray diffractometer (XRD) and Fourier Transform Infrared (FTIR) techniques.

2 Materials and methods

2.1 Synthesis of hydroxyapatite from eggshells

The three-step wet chemical precipitation method involves the following;

2.1.1 Extraction of calcium oxide from eggshells

Eggshells from Layer's chicken breed were domestically sourced for from-home consumption. The procedure for extracting calcium oxide from eggshells was adapted from the studies of Eric et al. [8] and Mohadi et al. [26]. To begin the process, the eggshells underwent a thorough cleansing using distilled water, then dried in an oven at 105℃ for 2 hours. Next, a mortar and pestle were employed to grind the eggshells into a fine powder, further refined into a consistent texture utilizing an electric blender. To ensure uniform particle size within the range of 0-250 microns, the resulting powder underwent screening through a 60 mesh sieve. The final step involved subjecting the powdered eggshells to calcination at a temperature of 900℃ for 2 hours. This thermal treatment facilitated the conversion of calcium carbonate into calcium oxide, thereby generating carbon dioxide as waste, as illustrated by Equation (1). Additionally, the organic constituents within the eggshells underwent decomposition during this process.

$$CaCO_3\ yields \Rightarrow \quad CaO + CO_2;\ T = (900)\ ℃ \tag{1}$$

2.1.2 Synthesis of hydroxyapatite

Hydroxyapatite was synthesized using the procedure adapted from Adeogun et al. [12], Kamalanathan et al. [11], and Ćurković et al. [27]. Following the heat treatment, a precise quantity of calcium oxide was dispersed in distilled water and agitated using a magnetic stirrer for 30 minutes, forming calcium hydroxide, as depicted by Equation (2).

$$CaO + H_2O\ yields \Rightarrow \quad +Ca(OH)_2 \tag{2}$$

To achieve the desired stoichiometric calcium-to-phosphorus ratio of 1.667, a phosphoric acid solution (0.6M) was carefully introduced into a calcium hydroxide suspension at a controlled rate of 1 mL/min. The resulting mixture of reactants, comprising calcium hydroxide and phosphoric acid, was stirred for 2 hours, followed by an aging period of 6 hours. The pH level of the solution was measured utilizing a pH checker.
Additionally, separate sets of reactants were subjected to extended aging times of 16 and 24 hours to investigate the influence of aging duration on the resulting morphology. After stirring, a batch of reactants was filtered to serve as the control reaction (not left to age). Equation (3) is the hydroxyapatite formation reaction.

$$10Ca(OH)_2 + 6H_3PO_4\ yields \Rightarrow \quad Ca_{10}(PO)_4(OH)_2 + 18(H)_2O \qquad (3)$$

Finally, hydroxyapatite was separated from all the reaction batches by a centrifuge. The final product was washed twice to eliminate any excessive acid ions. It was dried for 2 h at 100°C.

2.1.3 Sintering of hydroxyapatite powder

The hydroxyapatite powder obtained through synthesis underwent a sintering process at a temperature of 1200°C for 2 hours [11].

2.1.4 Characterization of the synthesized hydroxyapatite powder

The crystallographic structure of the synthesized powder was investigated using X-ray diffraction (XRD) analysis. A 40 kV X-ray diffractometer with a Cu target operating at 30 mA was employed for this purpose. The scanning range was conducted in two stages, utilizing a continuous scan speed of 8°/min and a preset time of 0.15 sec per measurement.

Fourier Transform-Infrared Spectroscopy (FTIR) was employed to identify organic and inorganic functional groups within the as-synthesized hydroxyapatite. The measurements were conducted in transmission mode, utilizing a Schimadzu UV-2550 instrument from Japan, covering a mid-infrared range with wave numbers spanning from 400 cm-1 to 4000 cm-1. To prepare the samples for analysis, 2 mg of each specimen was mixed and compressed alongside 300 mg of KBr to form a sample pellet.

The method outlined by the Association of Official Analytical Chemists (AOAC, 2005) was followed for the mineral analysis. The minerals in the resulting solution were determined using an Atomic Absorption Spectrophotometer (AAS), with the specific instrument utilized being the Bulk Scientific Accuzy 211 model. The measured values were expressed in parts per million (mg/100 g). Calcium (Ca) quantification was achieved spectrophotometrically using a UV/Vis Spectrophotometer with a model of 752 N.

3 Results and discussion

The wet chemical precipitation method involving ortho-phosphoric acid was employed to synthesize hydroxyapatite (H_3PO_4) as a phosphate source. There was a significant color change as the raw eggshells transformed to calcium oxide (Figure 1(a)), indicating that carbon dioxide (CO_2) and other organic matter present in the eggshells have been eliminated.

Figure 1(b) shows a color change from light brown eggshells to black ash. This occurred after putting it into a furnace at 900°C for 2 h. The black color initially obtained results from the carbonization of the eggshell showing an incomplete calcination process. The resultant powder was whitish on further heating for 2 h at 900°C, as shown in Figure 1(c). This indicates the presence of calcium oxide and complete calcination. There was no volume

reduction between the raw eggshell and the obtained product. However, there was mass reduction when the ash was formed.

a b c

Fig. 1. (a)Pulverized raw eggshells (b) semi-calcinated eggshells (c) completely calcinated eggshells to calcium oxide

.

Overall, the XRD patterns displayed similarities to the characteristic peaks of HAp, although certain distinctions were observed (as depicted in Figure 2). Notably, the two dominant peaks at 26° and 32-34°, commonly associated with HAp identification, were present. Furthermore, the detection of HAp diffraction peaks at 25°, 33°, 40°, and 50° confirmed that the synthesized material indeed corresponded to HAp. [28]. As observed in Figure 2, the most prominent peak was at 26° only for all four samples at different aging times. This can be attributed to the phosphate source used for the synthesis and the presence of β- Tricalcium phosphate (TCP: $Ca_3(PO_4)_2$) owing to incomplete reaction and some side reactions that occurred during synthesis [11]. Significant observations were made regarding the XRD analysis, with a notable increase in peak heights and a reduction in peak width. These changes indicate enhanced crystallinity and an increase in crystallite size.

For the analysis of functional groups present in the synthesized HAp, the FTIR absorption spectra, as demonstrated in Figures 3a-c, were examined. The spectra revealed distinctive absorption bands associated with the various vibrational modes of the phosphate (PO43-), hydroxyl (OH), and carbonate (CO_3) groups, thereby confirming the presence of carbonated HAp. Noteworthy peaks from the tetrahedral phosphate group within HAp were identified at 567.8 cm^{-1}, 608.9 cm^{-1}, 1115.57 cm^{-1}, and 1007.9 cm^{-1}. Furthermore, the stretching vibration of the OH group of HAp was responsible for the range of 3500 cm^{-1} to 3642 cm^{-1}, while the bands at 1638 cm^{-1} and 2550 cm^{-1} corresponded to adsorbed water molecules [12]. The presence of these bands ascertains the proper formation of hydroxyapatite from eggshells.

——— H1: XRD patterns of Hydroxyapatite obtained after aging for 0 hours

——— H2: XRD patterns of Hydroxyapatite obtained after aging for 6 hours

——— H3: XRD patterns of Hydroxyapatite obtained after aging for 16 hours

——— H4: XRD patterns of Hydroxyapatite obtained after aging for 24 hours

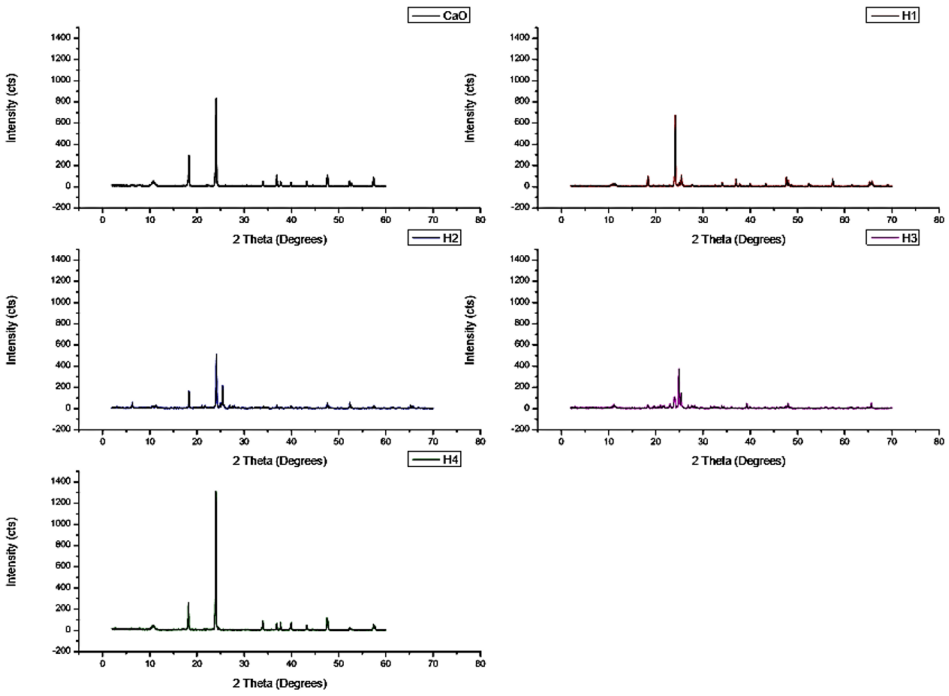

Fig. 2. XRD Patterns of obtained Hydroxyapatite samples

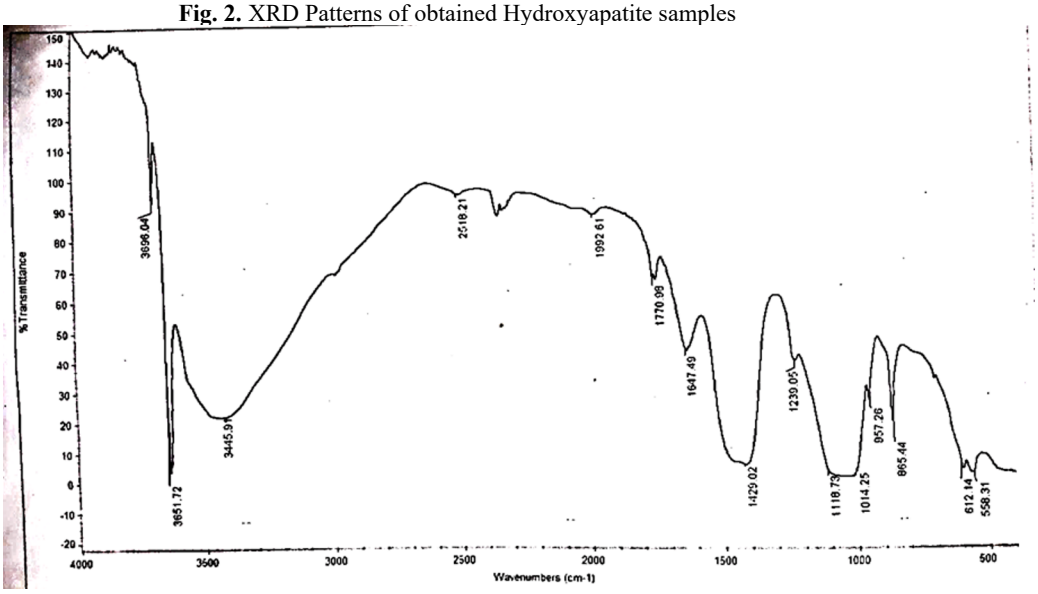

Fig. 3. (a): FTIR for HAp left to age for 0 hours

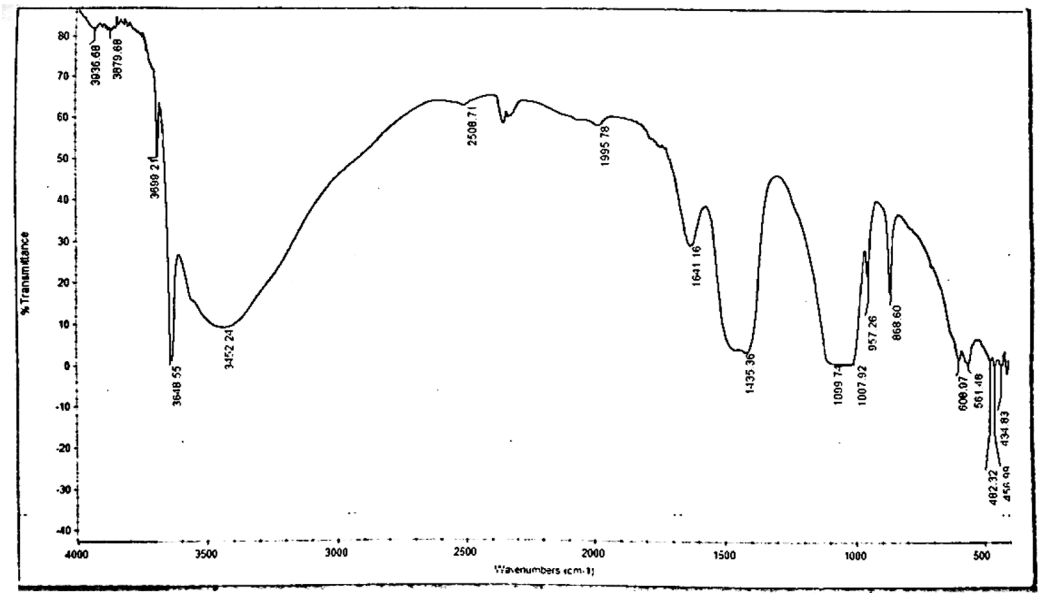

Fig. 3. (b) FTIR for HAp left to age for 6 hours

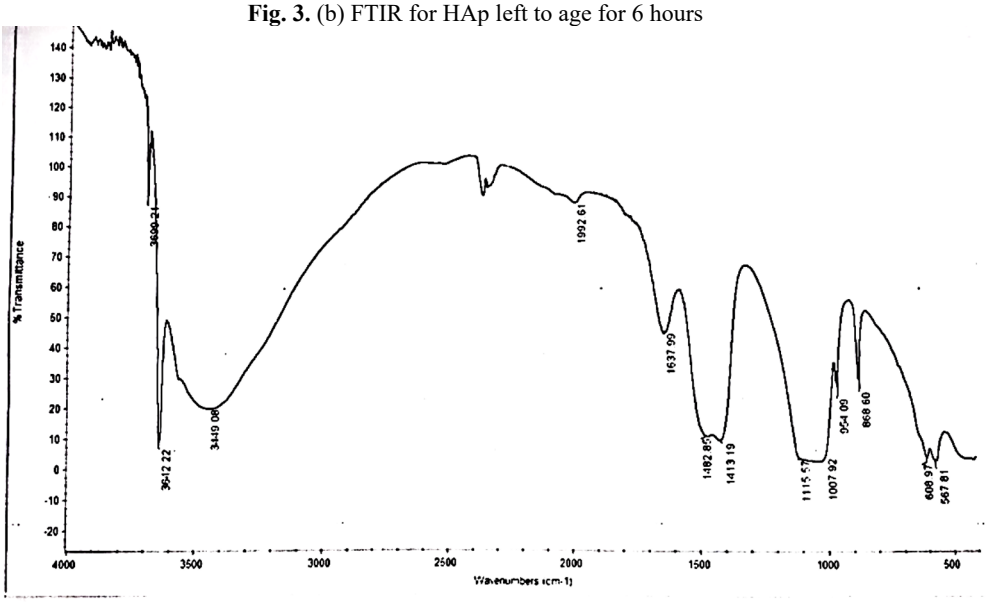

Fig. 3 (c) FTIR for HAp left to age for 24 hours

Table 1 shows the Ca/P ratio for various aging times obtained from the composition analysis. At the aging time of 24 hours, the Ca/P ratio was close to the stoichiometric value of HAp (1.67).

At lower aging times, 0 and 6 h, un-reacted CaO was observed. At longer aging times, the β-TCP phase was observed. This correlates with the observations of [13].

Table 1. Ca/P ratio of hydroxyapatite obtained from various aging times

Aging time (Hours)	Ca/P ratio	Observed Phases
0	1.9561	HAp + CaO
6	1.8214	HAp + CaO
16	1.6981	HAp + β-TCP
24	1.6815	HAp + β-TCP

4 Conclusion

Wet chemical precipitation has proven to be an effective method for successfully synthesizing hydroxyapatite from raw eggshells. Observations show that calcining at 900°C for 4 h converts the eggshells to calcium oxide. The optimum aging time for synthesizing hydroxyapatite by adding phosphoric acid to a solution of calcium oxide in water was 24 h. The reaction occurred at a pH above 8 to stabilize the precipitated HAp. The Ca/P ratio, which is close to stoichiometric HAp (1.67), was observed at the aging time of 24 h. However, β-Tri Calcium Phosphate ($Ca_3(PO_4)_2$) was found to have formed at various intervals owing to the incomplete transformation of calcium oxide to HA.

References

1. Y. Oshida, E.B. Tuna, O. Aktören, K. Gençay, Int. J. Mol. Sci. **11**, 1580–1678, (2010). https://doi.org/10.3390/ijms11041580.
2. C. Agrawal, J. Ong, M. Appleford, G. Mani, Cambridge University Press, (2013). https://doi.org/10.1017/cbo9781139035545.
3. K. Prabakaran, A. Balamurugan, S. Rajeswari, Bull. Mater. Sci. **28,** 115–119, (2005) https://doi.org/10.1007/bf02704229.
4. A. Tillberg, B. Järvholm, A. Berglund, Dent. Mater. **24**, 940–943, (2008) https://doi.org/10.1016/j.dental.2007.11.009.
5. R Vaderhobli, Dent. Clin. North Am. **55**, 619–625, (2011) https://doi.org/10.1016/j.cden.2011.02.015.
6. I. Sopyan, M. Raihana, M. Hamdi, S. Ramesh, Proc., Springer Berlin Heidelberg, 333–336. (n.d) https://doi.org/10.1007/978-3-540-69139-6_85.
7. FAO, (2015). http://www.fao.org/docrep/013/al969e/al969e00.pdf.
8. E. Rivera, M. Araiza, W. Brostow, V. Castaño, J. Diaz-Estrada, R. Hernández, J. Rodriguez, Mater. Lett. **41**, 128–134, (1999) https://doi.org/10.1016/s0167-577x(99)00118-4.
9. D. Goloshchapov, V. Kashkarov, N. Rumyantseva, P. Seredin, A. Lenshin, B. Agapov, E. Domashevskaya, Ceram. Int. **39**, 4539–4549, (2013) https://doi.org/10.1016/j.ceramint.2012.11.050.
10. A Hamidi, M. Salimi, A. Yusoff, AIP Conf. Proc., (2017). https://doi.org/10.1063/1.4981867.
11. P. Kamalanathan, S. Ramesh, L. Bang, A. Niakan, C. Tan, J. Purbolaksono, H. Chandran, W. Teng, Ceram. Int. **40**, 16349–16359, (2014) https://doi.org/10.1016/j.ceramint.2014.07.074.
12. A. Adeogun, A. Ofudje, M. Idowu, S. Kareem, Waste and Biomass Valorization. **9,** 1469–1473, (2017) https://doi.org/10.1007/s12649-017-9891-3.
13. [13] S.-J. Lee, Y.-S. Yoon, M.-H. Lee, N.-S. Oh, J. Nanosci. Nanotechnol. **7**, 4061–4064, (2007) https://doi.org/10.1166/jnn.2007.067.
14. W. Suksomran, R. Molloy, Sci. Technol. **25**, 57–66, (2017)
15. S.-C. Wu, H.-C. Hsu, S.-K. Hsu, Y.-C. Chang, W.-F. Ho, J. Asian Ceram. Soc. **4**, 85–90, (2016) https://doi.org/10.1016/j.jascer.2015.12.002.
16. N. Mohd-Pu'ad, J. Alipal, H. Abdullah, M. Idris, T. Lee, Mater. Today Proc. **42**, 172–177, (2021) https://doi.org/10.1016/j.matpr.2020.11.276.

17. G. Gergely, F. Wéber, I. Lukács, A. Tóth, Z. Horváth, J. Mihály, C. Balázsi, Ceram. Int. **36**, 803–806, (2010) https://doi.org/10.1016/j.ceramint.2009.09.020.
18. A. Pal, S. Maity, S. Chabri, S. Bera, A. Chowdhury, M. Das, A. Sinha, Biomed. Phys. Eng. Express., **3**, (2017) https://doi.org/10.1088/2057-1976/aa54f5.
19. D. Patel, M.-H. Kim, K.-T. Lim, J. Biosyst. Eng. 44, 128–133, (2019) https://doi.org/10.1007/s42853-019-00017-x.
20. A. Shavandi, A.E.-D.A. Bekhit, A. Ali, Z. Sun, Mater. Chem. Phys., **149–150**, 607–616, (2015) https://doi.org/10.1016/j.matchemphys.2014.11.016.
21. S. Jadalannagari, S. More, M. Kowshik, S. Ramanan, Mater. Sci. Eng. C. **31**, 1534–1538, (2011) https://doi.org/10.1016/j.msec.2011.07.001.
22. Y. Azis, M. Adrian, C. Alfarisi, Khairat, R. Sri, IOP Conf. Ser. Mater. Sci. Eng. **345**, (2018) https://doi.org/10.1088/1757-899x/345/1/012040.
23. S. Abidi, Q. Murtaza, J. Mater. Sci. Technol. **30**, 307–310, (2014). https://doi.org/10.1016/j.jmst.2013.10.011.
24. Y. Azis, N. Jamarun, S. Arief, H. Nur, J. Chem. **31**, 1099–1105, (2015) https://doi.org/10.13005/ojc/310261.
25. G. Krishnan, L. Babu, R. Pradhan, S. Kumar, Mater. Res. Express. **7**, (2020).
26. R. Mohadi, K. Anggraini, F. Riyanti, A. Lesbani, J. Environ. **1**, 32–35, (2016) https://doi.org/10.22135/sje.2016.1.2.32-35.
27. L. Ćurković, I. Žmak, S. Kurajica, M. Tonković, Z. Šokčević, M. Renjo, Materwiss. Werksttech. **48**, 797–802, (2017) https://doi.org/10.1002/mawe.201700052.
28. P. Piantone, F. Bodénan, R. Derie, G. Depelsenaire, Waste Manag. **23**, 225–243, (2003) https://doi.org/10.1016/s0956-053x(01)00058-7.